Heliyon 12 (2026) e44368

Contents lists available at ScienceDirect

Heliyon

journal homepage: www.cell.com/heliyon

Research article

Effect of prechlorination prior to activated carbon adsorption on trihalomethanes formation during final disinfection

Oriol Gibert [a,*], José Luis Beltrán [b], Joan de Pablo [a,c]

[a] Department of Chemical Engineering and Barcelona Research Center for Multiscale Science and Engineering, EEBE, Universitat Politècnica de Catalunya (UPC)-BarcelonaTECH, Av. Eduard Maristany 10-14, Barcelona, 08930, Spain
[b] Departament d'Enginyeria Química i Química Analítica, Universitat de Barcelona, Martí i Franquès 1-11, Barcelona, 08028, Spain
[c] EURECAT, Centre Tecnològic de Catalunya, Plaça de la Ciència 2, Manresa, Barcelona, 08243, Spain

ARTICLE INFO

Keywords:
Chlorination
Dissolved organic matter (DOM)
Granular activated carbon (GAC)
Trihalomethanes (THM)
Fluorescence excitation-emission matrix (EEM)

ABSTRACT

Granular Activated Carbon (GAC) is commonly used in water treatment for the removal of Dissolved Organic Matter (DOM) and diminution of the formation of Disinfection By-Products (DBP) during final disinfection. The aim of the present study was to evaluate whether prechlorination prior to GAC affected the character of DOM and could result in a decrease of trihalomethanes (THM) levels in finished water when postchlorination was applied. DOM character was analysed by fluorescence Excitation-Emission Matrices coupled to Parallel Factor Analysis (EEM + PARAFAC). Four different waters (three synthetic solutions containing structurally diverse model and identifiable fluorescent DOM -tyrosine, tryptophan, and humic substances- and real groundwater) were treated and compared. The solutions were sequentially subjected to prechlorination (at three different NaClO doses: 0, 4, and 8 mg/L), GAC adsorption, and posthclorination. The results showed that applying prechlorination prior to GAC adsorption resulted in lower concentrations of THM in postchlorinated water in comparison to the traditional practice of applying chlorination only after the GAC stage. The dose of 4 mg/L NaClO minimised the levels of THM in the finished water. The results also revealed that the fulvic-like EEM + PARAFAC component C1G (with λ_{exc} = 240 and 325 nm, and λ_{em} = 405 nm) showed a high correlation with THM levels and therefore appeared to be a very good predictor for THM formation. While promising with groundwater, this new approach to control THM in chlorinated finished water should be tested with water sources containing DOM with different properties before raising the technology readiness levels to pilot and real full-scale treatment trains.

1. Introduction

Dissolved organic matter (DOM) has long been recognised as a major precursor for harmful disinfection by-products (DBP) formation during water disinfection, which is performed in Drinking Water Treatment Plants (DWTPs) commonly by applying a chlorine-based disinfectant (e.g. sodium hypochlorite, NaClO) to the produced water in order to inactivate pathogenic microorganisms prior to distribution [1–3]. Among the DBP, trihalomethanes (THM) (followed by haloacetic acids HAA) are the most abundant ones [1,2] and, because of their potential carcinogenicity, the European Union has set a limit value for the four regulated THM of 100 μg/L [3]. In general, the higher the concentration of DOM and the higher the chlorine dosage in prechlorination, the higher the formation of THM

* Corresponding author.
E-mail address: oriol.gibert@upc.edu (O. Gibert).

https://doi.org/10.1016/j.heliyon.2025.e44368
Received 30 April 2024; Received in revised form 12 November 2025; Accepted 9 December 2025
Available online 17 December 2025

[4–6]. For this reason, the removal of DOM through adsorption onto Granular Activated Carbon (GAC) before disinfection is a current strategy to minimize DBP formation.

However, the formation of DBP depends not only on DOM concentration but also on its character. Consequently, DOM characterisation approaches have been developed to provide more valuable insights into DOM character than those provided by traditional surrogate parameters such as DOC, UVA_{254}, and SUVA, which continue to be the sole ones routinely monitored in most water treatment plants although they sometimes fail to predict the reactivity of DOM [7–9]. These approaches include DOM fractionation according to the hydrophobicity of organic compounds using XAD resins [1,7,9,10], or to the molecular size of organic compounds by means of successive UF membranes [7,9–11] or size exclusion chromatography (SEC) [11,12]. Thus, additional information on the physicochemical characteristics of DOM (grade of hydrophobicity/hydrophilicity and molecular weight distribution) can be obtained. Different degrees of success and sometimes contradictory conclusions have been obtained from the application of these approaches when trying to correlate DOM fractions and their reactivity. For instance, it has been reported that hydrophobic compounds form more DBP than the hydrophilic ones [1,13,14], although this may be true only for certain DBP [9,10], and that low molecular weight organics tend to generate the greatest DBP concentration [10,11,15]. By fractionating DOM by SEC, Hidayah et al. [12] conjectured that hydrophilic compounds might be the major precursor for THM while hydrophobic humic substances for HAA. Drawbacks in implementing the above-mentioned DOM characterisation techniques have been identified, and include difficulties in defining fractions with well-defined properties, interferences during fractionation, complications in analysing low concentrations of DOM, laborious procedures, significant costs, and, importantly from a point of view of full-scale applications, unfeasibility for on-line monitoring [8, 16].

Fluorescence spectrometry has emerged as a powerful tool for DOM characterization with potential to overcome these drawbacks. Fluorescence Excitation-Emission Matrices (EEM) allow to categorise fluorescent DOM (fDOM) into different fluorophores groups according to their emission and excitation wavelengths. These groups are typically associated to humic/fulvic-like fluorescent compounds and protein-like (tryptophan-like and tyrosine-like) compounds [17]. EEM offers several advantages over other characterisation techniques including low detection limits, high sensitivity (10–1000 higher than that of UVA_{254}), small sample volume required, robustness and rapidity, and the possibility of in-line monitoring [18,19]. The relatively large datasets resulting from EEM can be further processed using various mathematical treatments. Among them, Parallel Factor Analysis (PARAFAC) has drawn attention in the last years [20]. PARAFAC decomposes arrays of EEMs into groups of fluorophores with common excitation-emission signatures, termed components [21].

There is a relatively abundant body of studies focusing on the relation between EEM fluorophores and DBP formation during water treatment [22–24]. Humic- and fulvic-like fluorophores have been reported to be main precursors of carbonaceous DBP (C-DBP) including THM and HAA [6,8,25–29], suggesting that unsaturated and aromatic fluorescent structures typically found in humic and fulvic substances are more prone to react and incorporate chlorine, leading to the formation of THM and HAA, in comparison to other DOM structures [30]. In contrast, the formation of nitrogenous DBP (N-DBP) such as haloacetonitriles (HAN) has been found to exhibit various degrees of linear relationships across all fluorophore regions, also with protein-like fluorophores (e.g. tryptophan-like, tyrosine-like) [24,28,31]. The role played by less hydrophobic protein-like components with smaller molecular in N-DBP formation compared to humic- and fulvic-like materials is explained by the differences in the formation mechanisms leading to C-DBP and N-DBP [32].

However, only a few studies have included prechlorination prior to GAC in their treatment scheme, and often without addressing explicitly and deeply its effect on DBP formation [5,33–35] or without including GAC filtration in their treatment [36]. These scarce studies have reported that prechlorination prior to GAC adsorption stage can result in a decrease of DBP formation in comparison to non-prechlorination conditions [37,38], although it is not clear under what scenarios this is certain. Jiang et al. [37] found that levels of DBP and intermediate aromatic halogenated DBP in finished water were lower when NaClO was applied prior to the GAC stage. Raw water consisted in a synthetic solution of a commercial humic acid (3.0 mg/L DOC), and monitoring was based on the analysis of DOC, total organic halogen (TOX), THM and HAA, and polar halogenated organic compounds by electrospray ionization-triple polar quadrupole mass spectrometry (ESI-tqMS). Fischer et al. [39] also reported a decreased formation of DBP when prechlorination was applied prior to GAC, but also that this decrease depended on the type of DBP. Raw water consisted in coagulated and ultrafiltrated water from a DWTP (2.6–3.8 mg/L DOC), and DOM was fractionated by SEC. Results indicated that prechlorination followed by GAC preferentially removed low-molecular-weight DOM. Curthbertson et al. [38] also found that applying prechlorination could lead to an overall decrease of DBP formation in GAC-treated water, but with individual DBP even increasing in concentration. Raw water was collected from three different DWTPs (1.5–2.1 mg/L DOC) and GAC was evaluated at different service lives, but DOM was not fractionated by any characterisation technique. Finally, Erdem et al. [40] also investigated the effect of prechlorination prior to GAC contactors on the formation of DBP after a second chlorination, focusing on the role of GAC characteristics (i.e. surface area, pore size and surface charge). Raw water used consisted in solutions of NOM isolates and EfOM from wastewater treatment plants with DOC adjusted to 2.0 mg/L. In concomitance with the mentioned studies, the authors observed a decrease of DBP in finished water when prechlorination was applied. They also observed that this benefit of prechlorination was higher with waters with higher SUVA.

Despite the valuable information provided by these studies, none of them applied EEM + PARAFAC, and some used synthetic solutions containing DOM isolates or model compounds, which may not represent the behaviour of DOM in real waters. The effect of prechlorination on the character and reactivity of DOM (particularly to GAC adsorption and propensity to form DBP) in real waters as tracked by EEM-PARAFAC remains largely unexplored.

Based on the context described above, the present study aimed at evaluating the effect of prechlorination on DOM character as analysed by EEM + PARAFAC and its propensity to subsequently adsorb onto GAC and form DBP when postchlorination was applied. In order to get insight into how this effect changed with DOM type, four different waters (three synthetic solutions containing

structurally diverse model and identifiable fDOM -tyrosine, tryptophan, and humic substances- and a real groundwater containing a mixture of different fDOM) were treated and compared. Three doses of NaClO for prechlorination were tested: 0, 4, and 8 mg/L. DOC and fDOC were analysed after prechlorination and adsorption. Finally, all produced waters were subjected to postclorination to assess their potential to form THM.

2. Materials and methods

2.1. Water matrix

Four different solutions were prepared to assess the effect of prechlorination and adsorption on DOM character and on the formation of THM by the postchlorination of the remaining DOM. Three of the four solutions were synthetic, containing respectively tryptophan (hereafter referred to as R), tyrosine (Y), and humic substances (H). These model substances were chosen for 1) ideally representing most DOM typically found in natural water, 2) having the potential to form DBP during chlorination, and 3) being structurally diverse, well identifiable and distinguishable by EEM. The fourth one was real groundwater collected from the aquifer of Sant Adrià de Besòs (Barcelona, Spain) (hereafter referred to as G) whose composition is given in Table 1. This groundwater was chosen for being an available hydric resource with huge potential for reclamation [35]. The collection of groundwater for this study was done in September 2022 from a well located in the centre of Sant Adrià de Besòs. The sampled aquifer is thus one in a densely populated area but, thanks to restoration activities of the Besòs river carried out in the last decades, it now shows relatively high water quality.

As DOC in G was found to be at a concentration of 2.0 mg/L (see Table 1), synthetic solutions R, Y, and H were all prepared to have a similar DOC concentration (between 2 and 3 mg/L) for better comparison. Y and R solutions were prepared by weighting appropriate amounts of L-tryptophan ($C_{11}H_{12}N_2O_2$) (Sigma-Aldrich, >98 %) and L-tyrosine ($C_9H_{11}NO_3$) (Sigma-Aldrich, >98 %) and dissolving them in Milli-Q® water (18 MΩ cm). H solution was prepared by diluting a previously analysed concentrated solution of humic substances (without a known chemical formula) (Sigma Aldrich) to get a final concentration of 2–3 mg/L. All solutions were filtered with pre-washed 0.22 μm nylon membrane filters (Filter-Lab) and stored at 4 °C to minimize changes in the constituents.

2.2. GAC properties and dose used

Granular activated carbon (GC900) was supplied by Chiemivall and had a surface area of 968.6 m^2/g (determined with an ASAP 2020 V3.01H instrument). It was selected based on previous studies that demonstrated its effectiveness in adsorbing DOM [35,41]. Prior to the experiments, GAC was washed thoroughly with copious amounts of Milli-Q® water to remove any leachable DOC or impurities. GAC dose for the experiments was selected as to remove a fraction of DOM whilst still leaving a sufficient (ca. 0.5 mg/L) residual DOC concentration to permit analysis of DOC and THM after postchlorination. For this purpose, preliminary trials were conducted in which 1 L of G was put in contact with 0.05, 0.5, 1.0, and 1.5 g of GAC and left to equilibrate for 24 h in the same conditions as in sorption experiments of the study (see section 2.3 below). DOC removal after sorption experiments is plotted in Fig. S1. In view of the results, a dose of 1.0 g was selected for further experiments.

2.3. Experimental procedure

Solutions Y, R, H, and G placed in clean 1-L bottles under headspace-free conditions at room temperature (22±1 °C) were

Table 1
Composition of the groundwater from the aquifer of Sant Adrià de Besòs (solution G).

Parameter	Concentration
pH	7.9
Cond (μS/cm)	1550.0
DOC (mg/L)	2.0
Na^+ (mg/L)	154.4
K^+ (mg/L)	15.9
Mg^{2+} (mg/L)	26.8
Ca^{2+} (mg/L)	141.5
Cl^- (mg/L)	211.2
SO_4^{2-} (mg/L)	136.6
HCO_3^- (mg/L)	399.1
NO_3^- (mg/L)	8.1
PO_4^{3-} (mg/L)	<3
Br^- (mg/L)	0.7
Mn (μg/L)	211.8
B (μg/L)	158.1
Al (μg/L)	43.6
As (μg/L)	25.2
Cu (μg/L)	6.1
Fe, Pb, Ni, Cd, Cr (μg/L)	<5

sequentially subjected to prechlorination, adsorption on GAC, and postchlorination as follows.

2.3.1. Prechlorination

For each solution, three different NaClO (Panreac, 10 % w/v) doses were spiked (0, 4, and 8 mg/L). These dose values fall within the typical range used in water treatment plants. After the spiking, the bottles were agitated continuously on an orbital shaker (JP Selecta Rotabit) for 30 min, after which measured chlorine residual was quenched with an excess (105–110 % of the required stoichiometric amount) of $Na_2S_2O_3$ (Panreac, >99 %). The prechlorination time used in this study (30 min) was larger than those usually applied in DWTPs (3–10 min). The reason is that prechlorination in this study did not aim to control algae growth but to alter (by oxidation) the DOM character and elucidate whether this alteration affected the formation of THM after adsorption on GAC and further chlorination. The prechlorination time of 30 min was based on the scarce published articles on the same topic [37,39,40]. Water volumes of 20 mL were taken for analysis of DOC and its character by EEM.

2.3.2. Adsorption

After the prechlorination step, 1.0 g of GAC was added into each bottle. The bottles were left on the orbital shaker for further 24 h to allow adsorption to reach the equilibrium. A volume of 20 mL was taken for analysis of DOC and its character by EEM.

2.3.3. Final chlorination

At the end of the adsorption period all solutions were filtered through pre-washed 0.22 μm nylon filters (Filter-Lab) to separate GAC particles from the solution. The solutions were transferred into cleaned 1 L bottles for final chlorination. Then, 4 mg/L NaClO were spiked to each bottle to represent final disinfection. After 30 min, chlorination was quenched with an excess of $Na_2S_2O_3$ and solutions were analysed for THM determination. The prechlorination time used in this study (30 min) was shorter than those applied in standardized methods in which waters are chlorinated at high doses and long incubation times to maximise the formation of DBP (but at conditions far from those in DWTP). The reason is that these tests were performed as a proof of concept to evaluate the effect of prechlorination on the formation of THM during final disinfection, leaving for further studies the adjustment of the conditions to real full-scale water treatment facilities. Previous studies have also applied 30 min for final disinfection after their treatment trains (starting with prechlorination) [5,15]. The THM formed in each bottle were anticipated to be influenced by 1) prechlorination (as it may alter the DOC nature), and 2) adsorption (as it may remove some already-formed DBP, intermediate halogenated DOM, and remaining DOM).

2.4. Water analysis

All water samples were filtered through pre-washed 0.22 μm nylon filters prior to analysis. The determination of dissolved organic carbon (DOC) was performed using a TOC-L Shimadzu organic carbon analyser by high temperature catalytic oxidation (HTCO). The non-purgeable organic carbon method was selected (ISO number method 8245). Analytical precision and accuracy were tested against Reference Material provided by the DOC-CRM program (University of Miami- D.A. Hansell). The detection limit was 50 μg/L.

EEM spectra were recorded on an Agilent Cary Eclipse fluorescence spectrophotometer, controlled by Cary Eclipse Scan Application version 1.2, using a PC running the Microsoft Windows 7 operating system. A 1 cm Hellma QS cuvette was employed, and the instrument settings were adjusted as follows: Excitation wavelength (λ_{exc}) range: 200–500 nm (step 5 nm, with 5 nm slit width); Emission wavelength (λ_{em}) range: 250–600 nm (step 5 nm, with 2.5 nm width for R solution, 5 nm width for Y solution, and 10 nm slit width for H and G solutions); Scan rate: 3000 nm/min. The photomultiplier tube voltage was set to 600 V. The spectrofluorometer was autozeroed before each analysis. Milli-Q® water was used as blank. The processed EEM spectra were then plotted using Origin Lab. Decomposition of the EEM spectra into their underlying chemical components was accomplished by PARAFAC analysis. Data treatment was performed using the DOMfluor Toolbox and N-way Toolbox [21] under the MATLAB environment (The MathWorks, Inc., Natick, LEVEL, USA). The number of fluorescence components was determined by examination of residual errors. Component spectra were also compared against the on-line repository of published fluorescence spectra OpenFluor (www.openfluor.org) to evaluate spectral matching and component identification [42]. The maximum fluorescence signal (F_{max}) of each PARAFAC component (in arbitrary fluorescence units, FU) was used to represent its relative concentration. It must be bear in mind that F_{max} depends on the concentration of the fluorophore but also on its molar absorptivity and quantum yield. Because the two latter are unknown a F_{max} signal cannot be converted to a concentration, and therefore F_{max} gives an estimation of the relative concentration of each component [43,44]. Each dataset consisted of 6 EEM spectra. Although a global model would be more robust, combining all datasets in one single model was not possible because 1) the slit widths were different for the different sets in order to optimize the signals, and 2) the compositions of the solutions were too different. On the other hand, it has been reported that EEM spectra can be affected by the presence of $Na_2S_2O_3$ at concentrations of 25 mg/L and 50 mg/L [45]. As $Na_2S_2O_3$ in this study was applied at a 5–10 % stoichiometric excess, the remaining concentration of $Na_2S_2O_3$ were very low and its effect on EEM spectra was expected to be very minor. This was corroborated in further assays in which groundwater was spiked with $Na_2S_2O_3$ at concentrations in the range of 1.0–4.0 mg/L, yielding EEM spectra with F_{max} intensities differing by <1 % (Fig. S2). The absence of effect of THM on EEM was also corroborated in additional assays, in which groundwater was spiked with 12 μg/L and 24 μg/L of two different THM ($CHCl_3$ and $CHBr_3$) (Aldrich, 99 % and 96 %, respectively) and a mixture of them. Again, all EEM spectra showed F_{max} intensities differing by <1 % (Fig. S3).

The concentration of the four regulated, most predominant THM ($CHCl_3$, $CHBrCl_2$, $CHBr_2Cl$, $CHBr_3$) was measured using a gas chromatography-mass spectrometry (GC-MS) system equipped with headspace injection (Trace GC and DSQII model MS equipped with a Triplus autosampler from Thermo Fisher Scientific Limited). The column used was a Zebron ZB-624Plus capillary column (60m

× 0.32 mm x 1.8 μm). The injector port, interface, and ion source temperatures were set at 220 °C, 250 °C and 200 °C, respectively. The optimized temperature was programmed as follows: the initial temperature was 60 °C with hold time of 2 min, then ramped at rate of 8 °C/min up to 220 °C at which it was held for 5 min. The gas used as a carrier was helium at constant flow of 1.8 mL/min.

NaClO was analysed by first reacting ClO^- with an excess of I^- (added as KI) (Sigma Aldrich, >99 %) under acidic conditions and subsequent titration of the generated I_2 with sodium thiosulphate ($Na_2S_2O_3$) (Panreac, >99 %).

3. Results and discussion

3.1. Synthetic R, Y, and H solutions

3.1.1. DOC

Fig. 1 shows the levels of DOC in treated solutions after prechlorination and adsorption steps. It can be seen that final DOC levels differed depending on the type of solution (R, Y, or H) but not on the NaClO dose applied during prechlorination. The ranges of DOC in the finished water were 0.7–0.8, 0.5–0.7, and 2.9–3.0 mg/L for the R, Y, and H solutions, respectively. The decrease in DOC in solution R (≈74 %) and Y (≈90 %) could be attributed mostly to adsorption onto GAC rather than to prechlorination. In fact, GAC is acknowledged as one of the most effective adsorbents for removing DOC from water, particularly for lower molecular-weight organic compounds that can access more easily the micropores of the GAC particles [33,46]. It can be speculated that the unchanged levels of DOC for solution H (<2 %) were due to the fact that humic compounds in this solution were large in size and their adsorption could be impeded by steric effects. SEC analysis to determine the size distribution of DOM in solution H and BET analysis to determine the pore size of GAC should be performed to confirm this hypothesis or to help identify whether other reasons than the steric effect play a role.

On the other hand, prechlorination, as any other oxidation process, can break large molecular weight DOM into smaller and less aromatic organic fragments, but with limited effect on net removal of DOM [15,22,47].

3.1.2. Effect of prechlorination on the formation of THM in the finished water

Fig. 2 shows the concentration of the four regulated THM ($CHCl_3$, $CHBrCl_2$, $CHBr_2Cl$ and $CHBr_3$) formed after postchlorination of synthetic solutions R, Y, and H previously prechlorinated with NaClO (at doses of 0, 4, and 8 mg/L) and contacted with GAC.

For all three synthetic solutions, $CHCl_3$ was the major THM formed (accounting for 85–99 % of the four THM), while brominated THM were only marginally formed. This was consistent with the fact that these synthetic solutions were prepared with water Milli-Q® water (free of Br^-).

THM concentrations in H solution were higher than in solutions R and Y (note the difference in scale of y-axis in Fig. 2a, b, and c). This is due to the higher DOC concentrations after GAC adsorption (2.9–3.0 mg/L in solution H, vs < 1 mg/L in solutions R and Y), but also to the higher propensity of humic-like substances to form THM in comparison to amino acids such as tyrosine and tryptophan. The formation yield of THM by an organic compound is determined by the presence of functional groups susceptible to reaction with HClO. Being an electrophile, HClO reacts with electron-rich moieties (e.g. benzenes, phenols, methyl ketones) through a variety of reactions including oxidation, addition and electrophilic substitution reactions [48]. It is acknowledged that THM are formed mainly through the known haloform reaction, whereby methyl ketone groups (originally in NOM or formed during chlorination e.g. by opening of an aromatic ring) react with HClO to form THM following a series of reactions of enolizable compounds [48]. Although it is not possible to

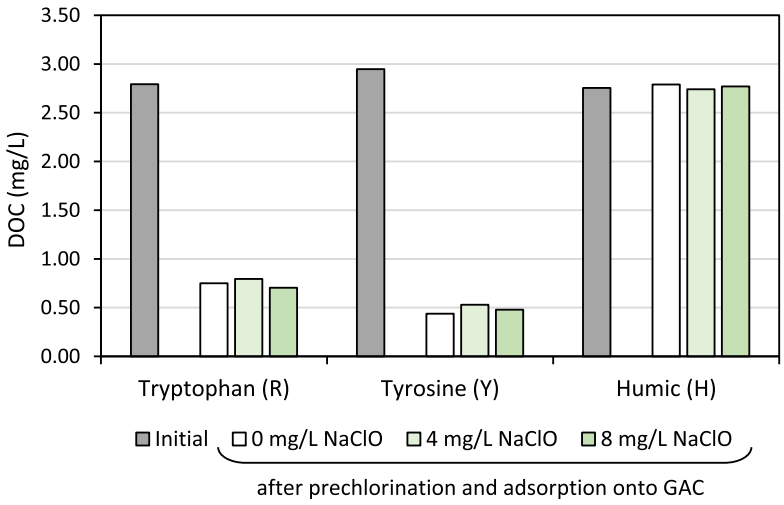

Fig. 1. Changes in DOC after prechlorination and adsorption onto GAC for the synthetic tryptophan-containing R solution, tyrosine-containing Y solution, and humic-containing H solution.

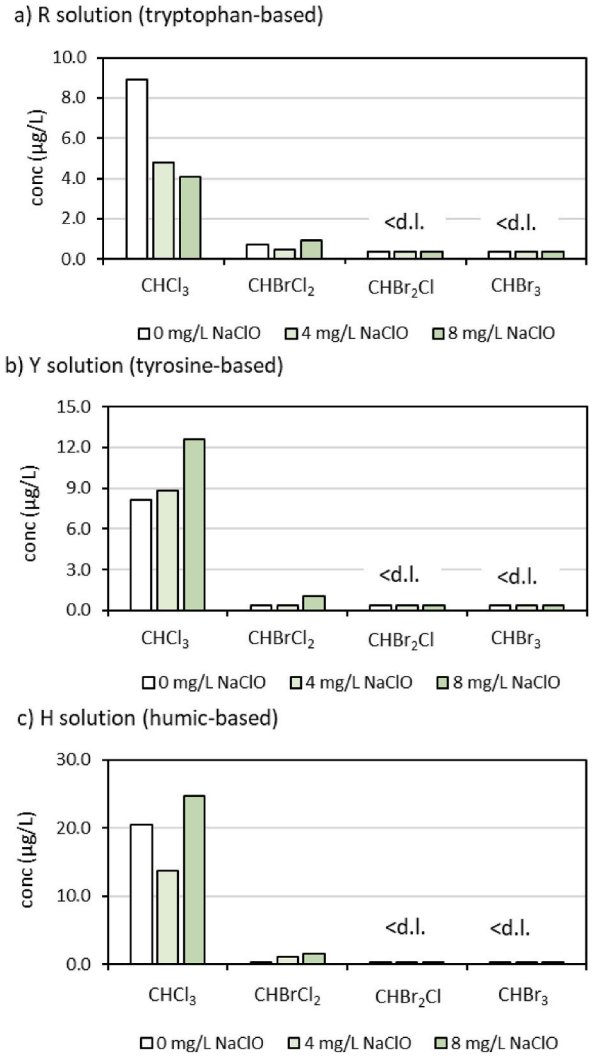

Fig. 2. Concentration of the four regulated THM ($CHCl_3$, $CHBrCl_2$, $CHBr_2Cl$, and $CHBr_3$) formed after postchlorination of synthetic solutions R, Y, and H previously prechlorinated with NaClO (at doses of 0, 4, and 8 mg/L) and contacted with GAC (<d.l.: below detection limit).

represent natural aquatic humic material by a unique molecular structure, it is known that humic substances contain a complex mixture of aromatic and aliphatic hydrocarbon structures with abundant functional groups including carboxylic acids, phenolic and alcoholic hydroxyls, and ketone groups that explain their high potential to form DBP [48], as observed for solution H in this study. Unlike many other amino acids, tryptophan and tyrosine contain aromatic rings and amino groups than can react with HClO and, although to a minor extent in comparison with humic substances, they too can act as THM precursors, as observed for solutions R and Y.

3.1.3. Effect of NaClO dose on THM formation

Considering that THM formation varied with the NaClO applied in the prechlorination while DOC did not, DOC did not seem to be a good parameter to anticipate the THM formation. Not all organic matter measured as DOC (at a mg/L level) acts as a precursor of THM (formed at a µg/L level), and therefore more sensitive analysis of organic compounds involved in THM formation is required.

Focusing on the effect of NaClO on THM formation, three different patterns were observed.

For R solution, THM formation in finished (i.e. postchlorinated) water decreased by 46 % and 54 % when NaClO during prechlorination was dosed at 4 and 8 mg/L, respectively. This finding was in line with those reported by Jiang et al. [37], Fisher et al. [39] and Erdem et al. [40].

The work of Jiang et al. [37] and Cuthbertson et al. [38] can help give an explanation to this pattern. In their study on the effect of prechlorination on adsorption of DOM onto GAC, Jiang et al. [37] analysed many polar halogenated DBP by means of a novel precursor ion scan (PIS) method using electrospray ionization triple quadrupole mass spectrometry (ESI-tqMS) and found that a wide variety of aromatic halogenated DBP formed during chlorination (the variety depending on the characteristics of DOM in water treated) and that

these intermediate DBP eventually decomposed and formed commonly known DBP (such as THM). They also observed that the various intermediate DBP, already formed THM, and unreacted DOM did not adsorb on GAC in the same way and extent, being this relative adsorbability onto GAC the main factor determining the DBP formation after prechlorination. The lowered DBP formation in finished water could then be explained by the fact that intermediate halogenated DBP formed during prechlorination were more easily adsorbed on GAC than DOM, in comparison to unchlorinated DOM. The authors attributed the enhanced adsorption of aromatic halogenated intermediate DBP to two factors: 1) they were lower in molecular weight and smaller in size, and therefore less affected by steric effects; and 2) they were more hydrophobic with higher affinity toward GAC. In line with this finding, Cuthbertson et al. [38] demonstrated not only the adsorption of already-formed intermediate aromatic halogenated DBP (or "preformed DBP" according to their own terminology) by GAC but also that TMHs formation potential in finished water decreased by approx. 60 % if prechlorination was applied prior to the GAC stage. With this in mind, the pattern of solution R shown in Fig. 2a can be interpreted as: chlorinated DOM likely adsorbed onto GAC more effectively than unchlorinated DOM, and therefore DBP formed after postchlorination decreased. This effect was more pronounced with the increase of the NaClO dosage employed during prechlorination.

Jiang et al. [37] also highlighted in their study that different trends can be observed "for a different source water with a different water matrix". In fact, for Y solution of the present study, the opposite trend was observed: THM formation increased with the applied NaClO dose (by 9 % and 55 % when applying 4 and 8 mg/L NaClO, respectively) (Fig. 2b). In this case prechlorination did not seem to favour the adsorption of DBP precursors but even to increase the THM-formation potential. In other words, contrarily to solution R, chlorinated DOM in solution Y seemed to be less prone to adsorption than unchlorinated DOM.

For H solution a more complex trend was observed, because a minimum of THM formation at the NaClO dose of 4 mg/L was observed (Fig. 1c). According to the reasoning followed so far, it would be concluded that prechlorination with a dose of 4 mg/L maximised the sorption of DBP precursors. This finding shared similarities with that of Zeng's et al. [49], who evaluated how chlorination affected the sorption of model proteins (serum album, lysozyme, adenylate kinase, and ribose-binding) and humic and fulvic acids (as analysed as DOC) onto a hydrophobic surface (graphene sheet) and found a maximum for humics and fulvics at a HClO dose of approximately 0.50 mmol HClO/mmol C, which is not far from our 4 mg NaClO/2.9 mg DOC/L (=0.23 mmol NaClO/mmol C). The discrepancy between these two values may be due to differences in the adsorbent used (graphene sheet vs. GAC in this study) and in the protein-model compounds tested.

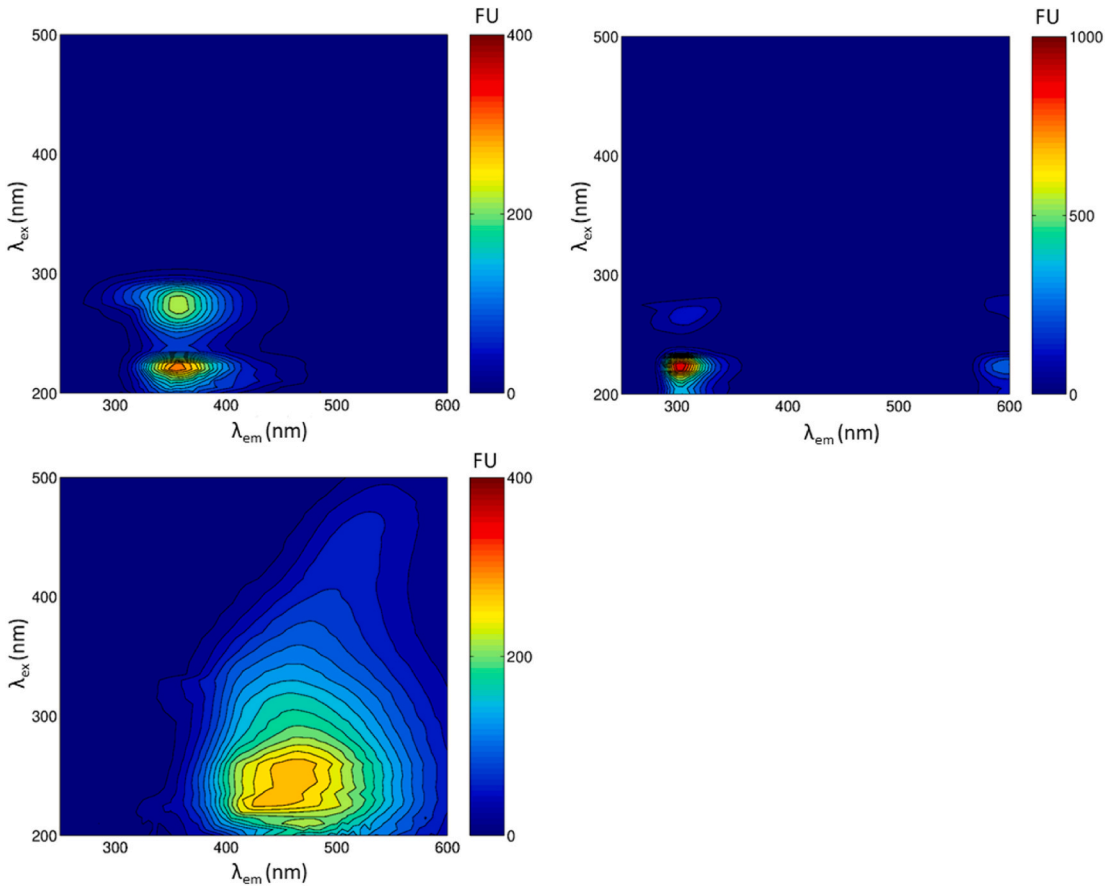

Fig. 3. Corrected EEM spectra for synthetic R, Y, and H solutions (fluorescence intensity in arbitrary fluorescence units, FU).

3.1.4. PARAFAC analysis of EEM spectra

DOM was monitored by EEM + PARAFAC after each stage (i.e. after prechlorination and after adsorption) in an attempt to identify whether PARAFAC-components were more related to THM formation than DOC. It must be underlined that not all DOM fluoresce, and therefore fDOC does not necessarily behave in the same way as DOC. For instance, DOC is decreased in principle only if there is a net removal of organic compounds (e.g. by adsorption), while fDOC can be decreased by a net removal of fluorescent organic compounds but also by transformation to non-fluorescent DOC.

Rayleigh and Raman scattering (1st and 2nd orders) were removed from EEM spectra [50] of solutions R, Y, and H (Fig. 3), and then they were decomposed using PARAFAC to get further insight into the fluorescent substances. The number of PARAFAC components provided by the selected model was 1, 1, and 4 for the solutions R, Y, and H, respectively. The excitation and emission wavelengths leading to the maximum fluorescence intensity (F_{max}) of each component, as well as its identification according to previous studies (OpenFluor) are shown in Table 2. As expected, fluorescence of solution R was clearly dominated by protein-like (tryptophan-type) fluorophores, that of solution Y by protein-like (tyrosine-type) fluorophores, and that of solution H by fulvic- and humic-like fluorophores (which are commonly present together because they usually contain the same fluorophores) [33].

3.1.5. Effect of prechlorination and adsorption on EEM-PARAFAC components

Fig. 4 shows the effect of prechlorination (with NaClO doses of 0, 4, and 8 mg/L) and subsequent adsorption onto GAC on F_{max} of each component for each synthetic solution (R, Y, and H). As can be seen, changes of fDOC differed depending not only on the nature of the DOM type but also, contrarily to DOC, on the NaClO dose applied during prechlorination. Prechlorination transformed a big fraction of fDOC into non-fluorescent DOC in solutions R and Y (decrease in F_{max} of C1R and C1Y by 50 % and 88 % at a NaClO dose of 4 mg/L, respectively, and >96 % for both solutions at a dose of 8 mg/L). This was not surprising, as it is known that smaller organic fragments generated by prechlorination often exhibit lower fluorescence than the original compounds [33,43]. Subsequent adsorption onto GAC completely removed all remaining fDOC in solutions R and Y (decrease in F_{max} of C1R and C1Y >90 %). Solution H showed different trends. fDOC remained fairly unchanged after prechlorination at the two NaClO doses. The decreases of F_{max} were <5 % for C1H (fulvic-like), C2H (humic-like) and C4H (humic-like). Only for C3H (humic-like) was a decrease of F_{max} by 20–25 % observed after NaClO exposure. Subsequent adsorption onto GAC hardly resulted in a decrease of F_{max} (overall decreases of F_{max} averaging 10 %) for C1H, C2H and C4H, with slightly higher decreases (around 30 %) for C3H. In all samples, pH ranged between 7.5 and 8.0, and therefore changes in fluorescence due to pH variations were considered minimal [36].

Judging from the results obtained with the synthetic solutions R, Y, and H, two preliminary conclusions could be anticipated: 1) prechlorination did not seem to substantially enhance adsorption of DOC nor of any EEM + PARAFAC component onto GAC, since differences between non-prechlorinated and prechlorinated samples were in call cases <10 %, and 2) THM levels in finished waters did not correlate with DOC or with any EEM + PARAFAC component ($R^2 < 0.5$).

3.2. Treatment of real groundwater

The same set of experiments was conducted with real groundwater from the aquifer in Sant Adrià del Besòs (solution G), whose composition was shown in Table 1. Unlike with solutions R, Y, and H, DOC and EEM were monitored at all treatment stages (i.e. after prechlorination and after GAC adsorption), as well as THM after postchlorination.

3.2.1. EEM analysis

Fig. 5 shows the EEM spectra for the G solution before exposure to NaClO (a), after exposure to NaClO at a dose of 4 mg/L (b) and 8 mg/L (c), and after adsorption on GAC of the prechlorinated samples (d, e, and f, respectively). Visual inspection of spectra reflected a moderate reduction in intensity of fluorescent peaks after prechlorination (a, b, and c), while the reduction was more pronounced after adsorption (d, e, and f).

The number of PARAFAC components provided by the model that best fitted the EEM spectra was 4. Fig. 6 plots the contour plots and the excitation and emission spectra of each of the four components. The excitation and emission wavelengths leading to the maximum fluorescence intensity (F_{max}) of each component, as well as its identification according to previous studies (OpenFluor) are shown in Table 3. Unlike solution R, Y, and H in which fluorescence was clearly dominated by only protein-like (tryptophan-type) fluorophores, only protein-like (tyrosine-type) fluorophores, and only fulvic- and humic-like fluorophores, respectively, natural groundwater (solution G) contained all types of these fluorophores.

Table 2
Excitation and emission maxima wavelengths and identification of the fluorescence PARAFAC components for each of the four solutions tested. The explained variance σ^2 for solutions R, Y, and H was 99.6 %, 99.8 % and 99.9 %, respectively.

Solution		λ_{exc} (nm)	λ_{em} (nm)	Identification
Synthetic R	C1R	220 and 275	335	Protein-like (tryptophan) [13]
Synthetic Y	C1Y	225 and 275	305	Protein-like (tyrosine) [31]
Synthetic H	C1H	245 and 325	415	Fulvic-like [13]
	C2H	250 and 365	475	Humic-like [13]
	C3H	215 and 450	530	Humic-like [17]
	C4H	210 and 315	445	Humic-like [17]

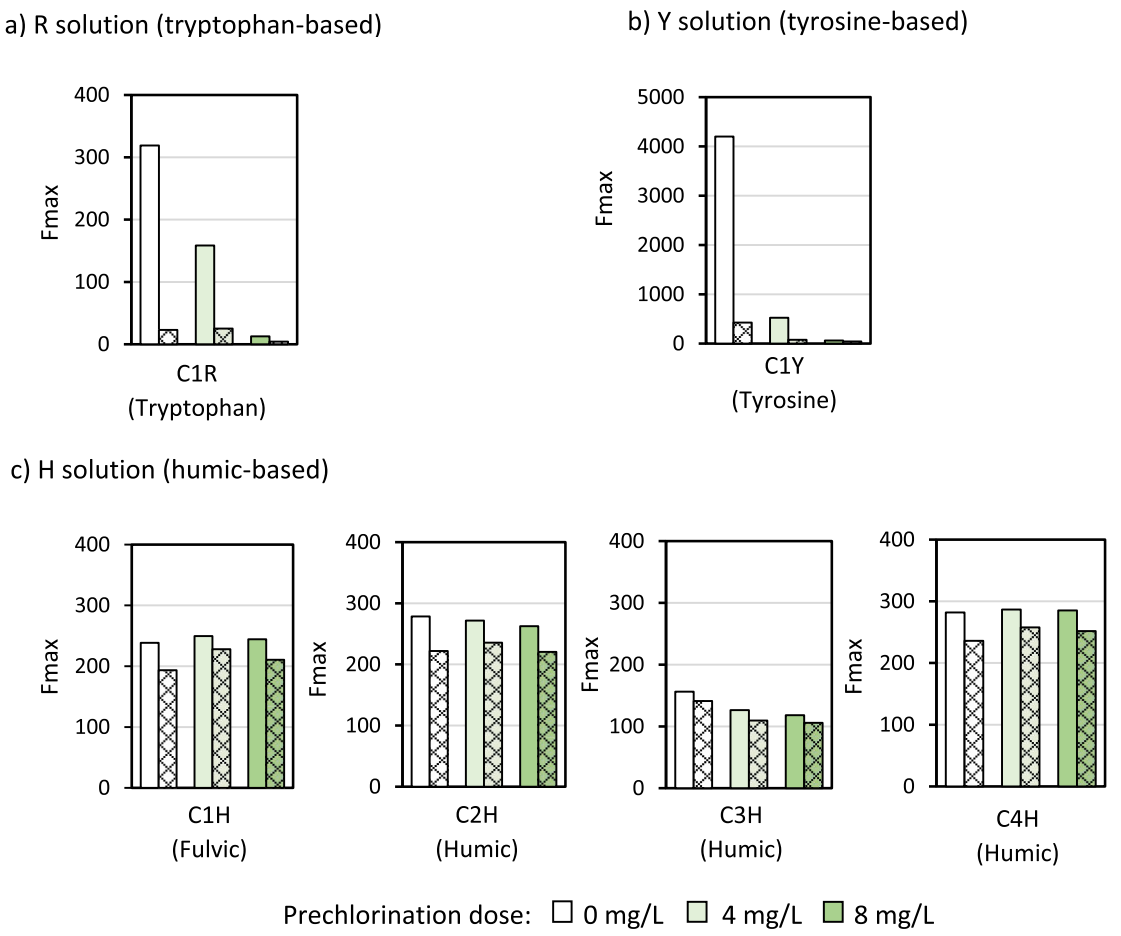

Fig. 4. Effect of prechlorination (with NaClO doses of 0, 4, and 8 mg/L) and subsequent adsorption onto GAC on EEM + PARAFAC components for synthetic solutions a) R, b) Y, and c) H. Solid bars represent F_{max} (in arbitrary fluorescence units) values for PARAFAC-components after prechlorination, while dashed bars after adsorption onto GAC.

3.2.2. Changes in DOM during treatment

Fig. 7 quantifies the effect of prechlorination (with NaClO doses of 0, 4, and 8 mg/L) and subsequent adsorption onto GAC on DOC and F_{max} of each component for groundwater (solution G).

As can be seen, DOC content was not affected at all by prechlorination (similarly to what was expected with the synthetic solutions R, Y, and H) but decreased by 55–61 % after adsorption, regardless of the NaClO applied during prechlorination. This latter finding made evident that, as observed with synthetic solutions R, Y, and H, prechlorination did not represent any substantial improvement in DOC removal. As lower molecular weight compounds are acknowledged to more easily diffuse into and adsorb onto pores of GAC [33, 46], the little effect of prechlorination might indicate that DOM in solution G likely consisted of low molecular weight and already prone to adsorption without need of breakdown down to smaller fragments. We hypothesize that if DOM had consisted in larger molecular weight compounds, prechlorination would have had a positive effect on DOM removal by GAC. It is also worth noting that a big difference was observed between the adsorbability of humic substances in synthetic solution H (<2 % removal) and that of humic substances in groundwater G (55–62 % removals). The reason of this difference might be the smaller size of humic substances in groundwater than in the synthetic solution H (and therefore their higher proneness to adsorption onto GAC), although other reasons not related to steric effects cannot be discarded.

With regard to fDOC, the overall removal for each component was 77 % (for C1G), 79 % (for C2G) and 82 % (for C3G), with most of it being due to adsorption while prechlorination had little effect. For the tyrosine-like matter (C4G), the low values of F_{max} signals since the beginning of the experiment made reliable interpretation of results difficult and trends could not be identified. Comparing against what was observed with the synthetic solutions R, Y and H, it must be underlined that components C1-C4G in groundwater G behaved differently with respect to the counterparts in synthetic solutions R, Y, and H in many aspects: first, fulvic and humic components in G (C1G and C2G) were not reduced by prechlorination (≤10 %, similarly to C1H and C2H) but they were by adsorption (differently from C1H and C2H). Again, differences were not observed at different NaClO doses during prechlorination (similarly to H solution). Second,

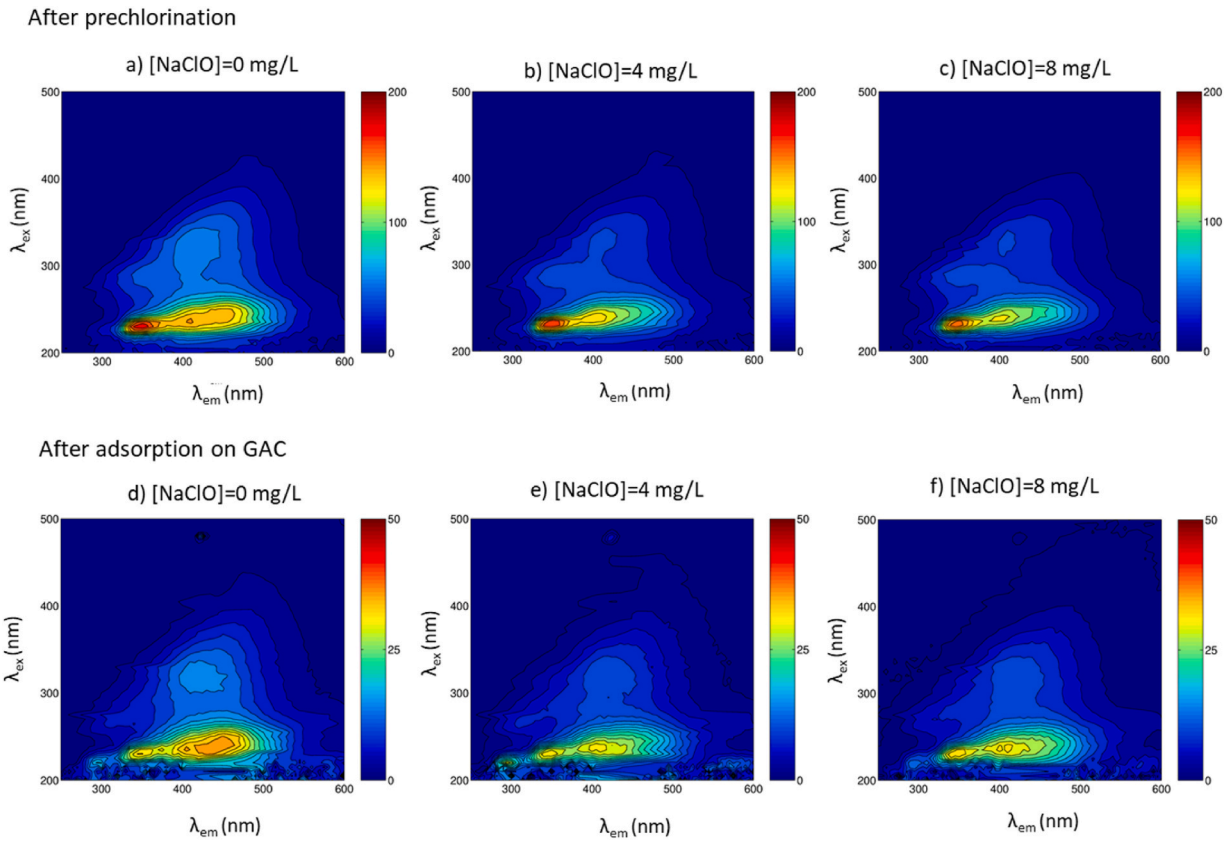

Fig. 5. EEM spectra for G solution before exposure to NaClO (a), after exposure to NaClO at a dose of 4 mg/L (b) and 8 mg/L (c), and after adsorption on GAC of the prechlorinated samples (d, e, and f, respectively).

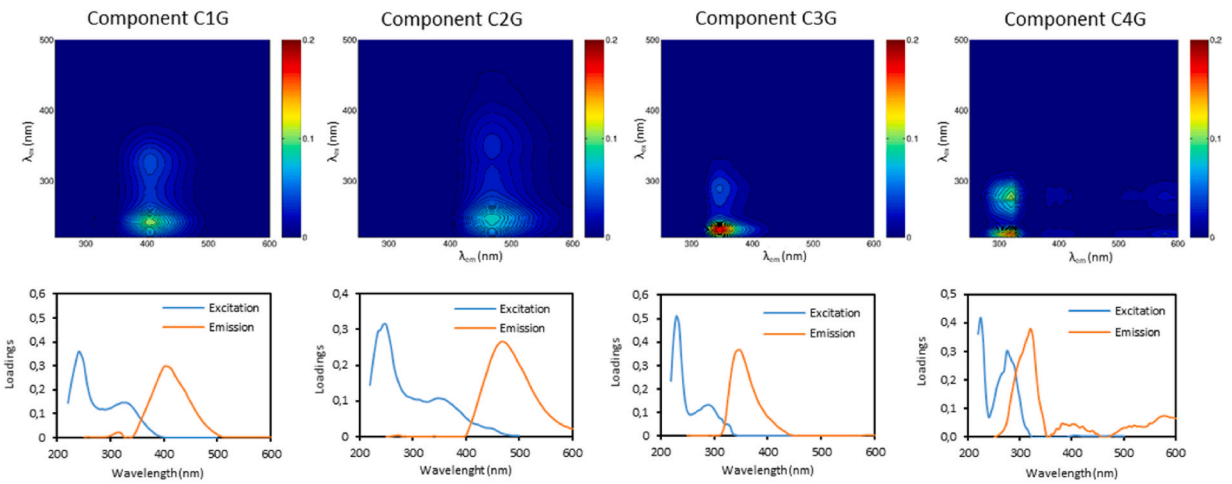

Fig. 6. Contour plots and loadings plots of components C1-C4G identified by PARAFAC analysis for groundwater (solution G).

for the tryptophan-like fluorophore (C3G) prechlorination did not result in F_{max} decreases (differently from C1R), but adsorption did, with F_{max} decreases of ≈80 % for all NaClO doses (similarly to C1R). These differences made evident that behaviour (or at least fluorescence behaviour) of model compounds used in synthetic solutions (isolated commercial tryptophan, tyrosine, and humics) does not reliably represent that of real tryptophan-like, tyrosine-like and humic-like fluorophores contained in real groundwater.

Table 3
Excitation and emission maxima wavelengths and identification of the fluorescence PARAFAC components for solution G. The explained variance σ^2 for solution G was 99.56 %.

Solution		λ_{exc} (nm)	λ_{em} (nm)	Identification
Groundwater G	C1G	240 and 325	405	Fulvic-like [13,34,36]
	C2G	245 and 350	470	Humic-like [13]
	C3G	230 and 290	345	Protein-like (tryptophan) [13,31,34]
	C4G	220 and 265	305	Protein-like (tyrosine) [34]

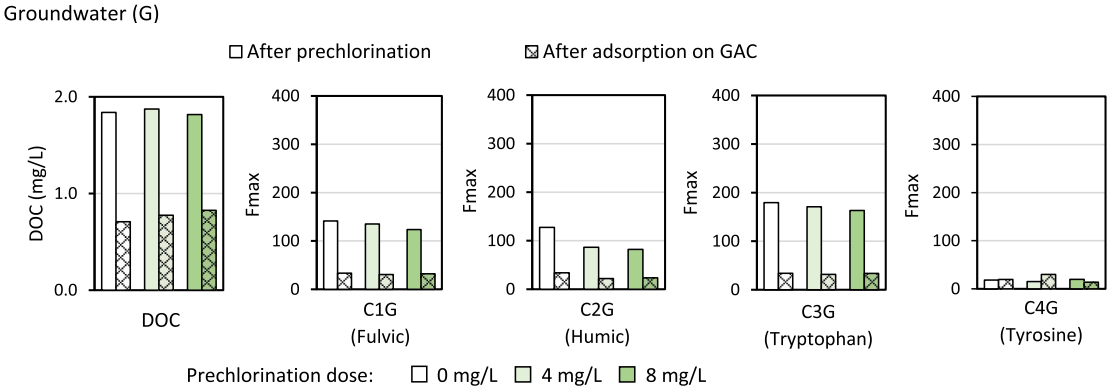

Fig. 7. Effect of prechlorination and subsequent adsorption on GAC on DOC and EEM-PARAFAC components for natural groundwater G. Filled bars represent DOC concentration and F_{max} values for PARAFAC components after prechlorination, while dashed bars after adsorption on GAC.

3.2.3. *Humics-to-proteins ration (HPR)*

A discussion on relative removal between humic-like and protein-like fractions by chlorination can be done by computing the ratio of the sum of F_{max} for humic-like fDOC components and the sum of F_{max} for protein-like fDOC components [24], hereafter termed HPR.

$$HPR = \frac{\sum F_{max}(humic-like\ fDOC)}{\sum F_{max}(protein-like\ fDOC)}$$

In this study, synthetic solutions R and Y only contained protein-like fDOC, while solution H only contained humic-like fDOC, and therefore such calculation could not be applied. Groundwater, however, contained both humic-like fDOC (components C1G and C2G) and protein-like fDOC (components C3G and C4G).

HPR decreased after prechlorination with 4 mg/L and 8 mg/L NaClO by approx. 13 % and 17 %, respectively, indicating slightly preferential removal of humic-like substances over protein-like (Fig. 8). Similar findings are reported by Maqbool et al. [51], who found that pre-oxidation of natural water (with NaClO but also $KMnO_4$ and O_3) decreased humic-like fluorescence more than protein-like. The authors explained this on the basis that humic-like aromatic structures were more prone to chemical oxidation than the large molecular-weight biopolymers including protein-like components. Similar patterns are reported by Baghoth et al., [43] when

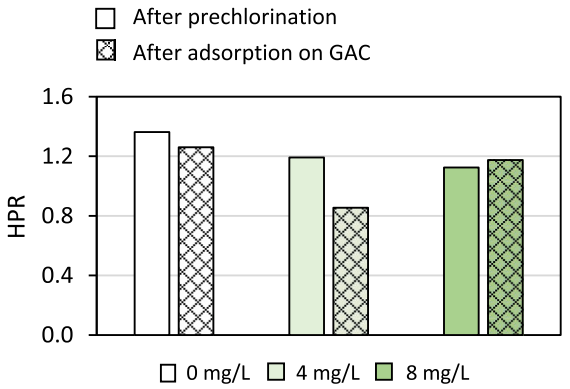

Fig. 8. Variation in the ratio between the humic-like and protein-like fDOC components (HPR) after prechlorination and adsorption on GAC.

preoxidising with O_3. Changes of HPR by adsorption onto GAC (computed by comparison of pre-adsorption and post-adsorption F_{max}) showed a decrease by 7 %, 28 %, and −4 %, indicating a preferential adsorption of humic-like over protein-like at the intermediate NaClO dose of 4 mg/L. This maximum is consistent with Zeng et al. [49], who observed an optimal NaClO dose for which adsorption of humic substances onto sheet graphene used as adsorbent was maximal. The reduction of HPR over the two-stage treatment (pre-chlorination and adsorption) was 7 %, 37 %, and 14 % for NaClO doses of 0, 4, and 8 mg/L, respectively, indicating preferential overall removal of humic-like over proteic-like.

3.2.4. Formation of THM

Fig. 9 shows the formation of THM after postchlorination of treated groundwater.

A major difference was clearly noted in comparison to synthetic solutions R, Y, and H: the presence of Br^- in groundwater shifted the formation of chlorinated THM (Cl-THM) to brominated THM (Br-THM). In fact, Br-THM accounted for 91 % of all THM. The formation of Br-THM over chloroform in Br^--containing water has been reported elsewhere [46,48] and can be quantified by the bromine incorporation factor (BIF), which is defined as follows for THM [4]:

$$BIF_{THM} = \frac{[CHBrCl_2] + 2 \cdot [CHBr_2Cl] + 3 \cdot [CHBr_3]}{[CHCl_3] + [CHBrCl_2] + [CHBr_2Cl] + [CHBr_3]}$$

BIF can range from 0 (when no brominated species have been formed) to 3 (when all THM are found as pure bromoform). The values of BIF_{THM} for groundwater G (from Fig. 9) averaged 2.24, which was higher than the average of 0.24 corresponding for synthetic solutions R, Y, and H (from Fig. 2).

The same consideration on relative reactivity of intermediate THM precursors, THM, and unreacted DOM discussed for the synthetic solutions apply for groundwater G, with the additional complexity posed by the presence of four THM instead of practically only $CHCl_3$ for synthetic solutions. In this case, the profile shown by all THM resembled that for H, probably because DOM in G resembled that in H. This is consistent with the fact that humic- and fulvic-substances tend to dominate in many surface and groundwaters [33]. This profile indicated a minimum formation of all Br-THM at intermediate pre dose of 4 mg/L, again in conformity with Zeng's et al. [49] as discussed above.

Recent studies have documented that quenching agents such as $Na_2S_2O_3$ used in this study have a decomposition effect on Total Organic Halogen (TOX), which is a surrogate bulk parameter that provides a measurement of the overall DBP, including THM analysed in this study [52]. Other studies have pointed out, however, that while this stands true for TOX and aromatic halogenated DBP such as halophenols, halonitrophenols and halobenzoquinones, $Na_2S_2O_3$ does not adversely affect the concentration of THM, with decreases of approx. 5 % [53].

Concentrations of THM were linearly correlated with signals for each component (F_{max}) measured prior to final chlorination in order to identify which PARAFAC component(s) contributed most to THM formation (Fig. 10).

It can be seen that the component that better correlated with ΣTHM concentration was C1G, with a $R^2 = 0.999$, followed by C3G ($R^2 = 0.886$) and C2G ($R^2 = 0.770$). Component C4G appeared to be not correlated with any THM, probably affected by the low levels of tyrosine ($R^2 = 0.489$). Of all components, only C1G presented statistically significant influence on the formation of ΣTHM (p-value $= 0.02 < 0.05$), while C2G, C3G and C4G did not (p-values$>$0.05).

The linear correlation factors (R^2) between each individual THM and F_{max} of EEM + PARAFAC components and the statistical significance as measured by associated p-values are given in Table 4.

Strong correlations were found between the concentration of $CHBrCl_2$, $CHBr_2Cl$ and $CHBr_3$ and the F_{max} of the fulvic-like C1G (with $R^2 \geq 0.94$), with the latter being statistically significant (p-value$<$0.05). The correlations decreased for PARAFAC components C2G and C3G. This suggested that fulvic-like C1G (with $\lambda_{exc} = 240$ and 325 nm, and $\lambda_{em} = 405$ nm) appeared to be a very good predictor for THM formation. This finding is in line with those reported by other researchers. Zhang et al. [23] observed a very good linear correlation ($R^2 = 0.90$) between DBP formation and the fluorescence intensity at $\lambda_{exc}/\lambda_{em} = 310/416$ nm, which is near the $\lambda_{exc}/\lambda_{em}$ pair of C1G of this study. Watson et al. [24] also observed a strong correlation between fluorophore with F_{max} at $\lambda_{exc}/\lambda_{em} = 240/400$ nm and highly-chlorinated THM (i.e. $CHCl_3$ and $CHBrCl_2$), with Spearman's coefficients in the range of 0.92–0.94 (but not for $CHBr_2Cl$ and $CHBr_3$, probably because of the lower Br^-/DOC ratios in their experiments). Finally, fairly high correlation factors ($R^2 = 0.84$) were observed between $CHCl_3$ formation and F_{max} for a fluorophore at $\lambda_{exc} = 238$ and 329 nm, and $\lambda_{em} = 430$ nm [8].

Two final considerations must be made with regard to the extrapolation of the results of this study to other scenarios. First, although the strong empirical correlation between the humic/fulvic like component C1G and ΣTHM has also been observed for other types of water sources different from groundwater (surface water, tap water, wastewater) [25], it must be bear in mind that other studies report minimal improvements of PARAFAC components in the prediction of the DBP production potential. This discrepancy may be due to the fact that DOM originating from different sources may exhibit distinct reactivity but yield similar fluorescence intensities. That being the case, other advanced analytical techniques, such as size exclusion chromatography (SEC) or high resolution-mass spectroscopy (HR-MS) may be needed to complement DOM characterisation.

Second, it is known that DOM fluorescence can be affected by the presence of metal ions, mainly through metal-DOM complexation. However, such alterations have been reported at metal ion concentrations much higher than those in groundwater from the aquifer of Sant Adrià de Besòs (Table 1). For instance, and concerning major ions, Chen et al. [54] observed a reduction of fluorescence intensity $<$10 % at concentrations as high as 27 mg/L NaCl, 5 g/L $MgCl_2$ and 1.1 g/L $CaCl_2$. With regard to minor transient metals, fluorescence intensity variation was observed minimal ($<$2 %) at concentrations of 0.8 and 1.5 mg/L Fe and 0.4 mg/L Al [55], or reduced by $<$20 % at Pb concentrations as high as 2 mg/L [54]. For all this, it was expected that fluorescence analysed in this study would not be affected

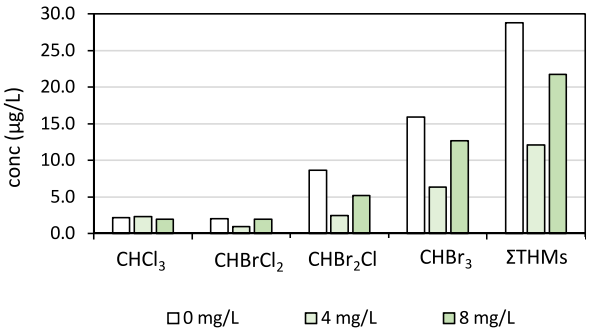

Fig. 9. Formation of THM after postchlorination of treated groundwater.

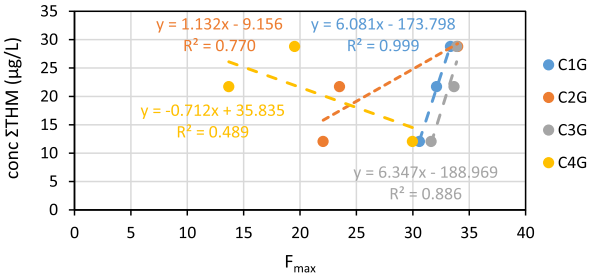

Fig. 10. Correlation of concentration of all THM formed and F_{max} (in arbitrary fluorescence units) of components C1G, C2G, C3G and C4G as analysed by EEM + PARAFAC.

Table 4
Linear correlation factors (R^2) between each individual THM and F_{max} of EEM + PARAFAC components and statistical significance as measured by associated p-values.

R^2 values (p-value)	$CHCl_3$	$CHBrCl_2$	$CHBr_2Cl$	$CHBr_3$
C1G (Fulvic-like)	0.01 (0.93)	0.97 (0.11)	0.94 (0.15)	**0.99 (0.04)**
C2G (Humic-like)	0.29 (0.63)	0.65 (0.41)	0.95 (0.15)	0.84 (0.26)
C3G (Tryptophan-like)	−0.07 (0.83)	0.96 (0.13)	0.67 (0.39)	0.82 (0.28)
C4G (Tyrosine-like)	0.44 (0.54)	−0.63 (0.42)	−0.23 (0.68)	−0.40 (0.56)

by the low levels of metals present in the groundwater of Sant Adrià de Besòs, but this could be the case if other water sources with a more complex matrix were used.

4. Conclusions

This study provides two particularly insightful findings that can be useful for water treatment plants aiming at minimising THM formation during disinfection.

On one hand, it has demonstrated that applying prechlorination prior to GAC adsorption can result in lower concentrations of THM in postchlorinated water in comparison to the traditional practice (i.e. applying chlorination after the GAC stage only). The reason is that pre-clorination can generate intermediate halogenated DBP precursors with higher proneness to adsorb onto GAC than unhalogenated DBP precursors. In this study, we found that prechlorination with NaClO at a dose of 4 mg/L maximised such adsorption (i.e. minimised the further THM formation after postchlorination). At this NaClO dose, the levels of THM formed during postchlorination were 58 % and 45 % lower than at NaClO doses of 0 and 8 mg/L, respectively.

On the other hand, EEM holds great potential in estimating THM formation and therefore in helping develop control strategies to reduce THM formation. The fulvic-like EEM + PARAFAC component C1G (with λ_{exc} = 240 and 325 nm, and λ_{em} = 405 nm) showed particularly a high correlation with THM levels (R^2 = 0.94–0.99) and therefore appeared to be a very good predictor for THM formation.

It must be recalled that EEM not only can provide more valuable information than traditional surrogates (e.g. DOC, SUVA) but also that it is simpler and more straightforward than other advanced techniques (e.g. SEC, resins fractionation), which are often laborious and demand a degree of skill. Moreover, and representing probably the most important advantage in comparison to the above mentioned advanced techniques, the EEM technique allows in-line monitoring of DOM in treatment plants. In fact, submersible fluorescence sensors have successfully been employed to track the removal of organic matter in water treatment systems in real-time

[56]. For all this, EEM emerges as an attractive tool for water utilities in drinking, purification and reclamation schemes.

CRediT authorship contribution statement

Oriol Gibert: Writing – original draft, Methodology, Investigation, Formal analysis, Conceptualization. **José Luis Beltrán:** Writing – review & editing, Validation, Methodology, Formal analysis. **Joan de Pablo:** Writing – review & editing, Validation, Project administration, Funding acquisition.

Data availability statement

Data will be made available on request.

Declaration of competing interest

The authors declare that they have no known competing financial interests or personal relationships that could have appeared to influence the work reported in this paper.

Acknowledgements

This study received funding from the European Regional Development Fund (FEDER) through the project PECT Litoral Besòs: Territori Sostenible (GO03-003358) and from the Research Spanish Agency (AEI) through the project SAFEWARE (PID2023-146999OB-I00). Support was also received from the Catalan AGAUR Agency through the Research Groups Support Programme (2021-SGR-GRC-00596) and from the AEI through the María de Maeztu Programme (CEX2023-001300-M/10.13039/501100011033). Authors also thank C. Ribalta for laboratory assistance and D. P. Orlando for EEM analyses.

Appendix A. Supplementary data

Supplementary data to this article can be found online at https://doi.org/10.1016/j.heliyon.2025.e44368.

References

[1] L. Liang, P.C. Singer, Factors influencing the formation and relative distribution of haloacetic acids and trihalomethanes in drinking eater, Environ. Sci. Technol. 37 (2003) 2920–2928, https://doi.org/10.1021/es026230q.
[2] N. Chaukura, S.S. Marais, W. Moyo, N. Mbali, L.C. Thakalekoala, T. Ingwani, B.B. Mamba, P. Jarvis, T.T.I. Nkambule, Contemporary issues on the occurrence and removal of disinfection byproducts in drinking water - a review, J. Environ. Chem. Eng. 8 (2020) 103659, https://doi.org/10.1016/j.jece.2020.103659.
[3] A.F. Gilca, C. Teodosiu, S. Fiore, C.P. Musteret, Emerging disinfection byproducts: a review on their occurrence and control in drinking water treatment processes, Chemosphere 259 (2020) 127476, https://doi.org/10.1016/j.chemosphere.2020.127476.
[4] Y. Hou, W. Chu, M. Ma, Carbonaceous and nitrogenous disinfection by-product formation in the surface and ground water treatment plants using Yellow River as water source, J. Environ. Sci. 24 (2012) 1204–1209, https://doi.org/10.1016/S1001-0742(11)61006-1.
[5] Z.-G. Niu, X.-P. Hu, Y. Zhang, Y.-Y. Su, Effect of chlorine dosage in prechlorination on trihalomethanes and haloacetic acids during water treatment process, Environ. Sci. Pollut. Res. 24 (2017) 5068–5077, https://doi.org/10.1007/s11356-016-8265-x.
[6] B. Manivannan, M. Borisover, Strengths of correlations with formation of chlorination disinfection byproducts: effects of predictor type and other factors, Environ. Sci. Pollut. Res. 27 (2020) 5337–5352, https://doi.org/10.1007/s11356-019-06976-0.
[7] Q.-S. Wei, C.-h. Feng, D.-s. Wang, B.-y. Shi, L.-t. Zhang, Q. Wei, H.-x. Tang, Seasonal variations of chemical and physical characteristics of dissolved organic matter and trihalomethane precursors in a reservoir: a case study, J. Hazard. Mater. 150 (2008) 257–264, https://doi.org/10.1016/j.jhazmat.2007.04.096.
[8] A.D. Pifer, J.L. Fairey, Improving on $SUVA_{254}$ using fluorescence-PARAFAC analysis and asymmetric flow-field flow fractionation for assessing disinfection byproduct formation and control, Water Res. 46 (2012) 2927–2936, https://doi.org/10.1016/j.watres.2012.03.002.
[9] G. Hua, D.A. Reckhow, I. Abusallout, Correlation between SUVA and DBP formation during chlorination and chloramination of NOM fractions from different sources, Chemosphere 130 (2015) 82–89, https://doi.org/10.1016/j.chemosphere.2015.03.0.
[10] N. Karapinar, V. Uyak, S. Soylu, T. Topala, Seasonal variations of NOM composition and their reactivity in a low humic water, Environ. Prog. Sustain. 33 (2014) 962–971, https://doi.org/10.1002/ep.11878.
[11] Z.-Y. Zhao, J.-D. Gua, H.-B. Li, X.-Y. Li, K.M.-Y. Leung, Disinfection characteristics of the dissolved organic fractions at several stages of a conventional drinking water treatment plant in Southern China, J. Hazard. Mater. 172 (2009) 1093–1099, https://doi.org/10.1016/j.jhazmat.2009.07.101.
[12] E.N. Hidayah, Y.-C. Chou, H.-H. Yeh, Using HPSEC to identify NOM fraction removal and the correlation with disinfection by-product precursors, Water Supply 16 (2016) 305–313, https://doi.org/10.2166/ws.2015.139.
[13] L. Yang, D. Kim, H. Uzun, T. Karanfil, J. Hur, Assessing trihalomethanes (THMs) and N-nitrosodimethylamine (NDMA) formation potentials in drinking water treatment plants using fluorescence spectroscopy and parallel factor analysis, Chemosphere 121 (2015) 84–91, https://doi.org/10.1016/j.chemosphere.2014.11.033.
[14] H. Sun, X. Song, T. Ye, J. Hu, H. Hong, J. Chen, H. Lin, H. Yu, Formation of disinfection by-products during chlorination of organic matter from phoenix tree leaves and *Chlorella vulgaris*, Environ. Pollut. 243 (2018) 1887–1893, https://doi.org/10.1016/j.envpol.2018.10.021.
[15] Y. Zhang, N. Zhang, P. Zhao, Z. Niu, Characteristics of molecular weight distribution of dissolved organic matter in bromide-containing water and disinfection by-product formation properties during treatment processes, J. Environ. Sci. 65 (2018) 179–189, https://doi.org/10.1016/j.jes.2017.03.013.
[16] D.M. Golea, A. Upton, P. Jarvis, G. Moore, S. Sutherland, S.A. Parsons, S.J. Judd, THM and HAA formation from NOM in raw and treated surface waters, Water Res. 112 (2017) 226–235, https://doi.org/10.1016/j.watres.2017.01.051.
[17] W. Chen, P. Westerhoff, J.A. Leenheer, K. Booksh, Fluorescence excitation-emission matrix regional integration to quantify spectra for dissolved organic matter, Environ. Sci. Technol. 37 (2003) 5701–5710, https://doi.org/10.1021/es034354c.

[18] R.K. Henderson, A. Baker, K.R. Murphy, A. Hambly, R.M. Stuetz, S.K. Khan, Fluorescence as a potential monitoring tool for recycled water systems: a review, Water Res. 43 (2009) 863–881, https://doi.org/10.1016/j.watres.2008.11.027.

[19] J. Bridgeman, M. Bieroza, A. Baker, The application of fluorescence spectroscopy to organic matter characterisation in drinking water treatment, Rev. Environ. Sci. Biotechnol. 10 (2011) 277–290, https://doi.org/10.1007/s11157-011-9243-x.

[20] D. Markechová, M. Tomková, J. Sádecká, Fluorescence excitation-emission matrix spectroscopy and parallel factor analysis in drinking water treatment: a Review, Pol. J. Environ. Stud. 22 (2013) 1289–1295.

[21] C.A. Andersson, R. Bro, The N-way toolbox for MATLAB, Chemometr. Intell. Lab. Syst. 52 (2000) 1–4, https://doi.org/10.1016/S0169-7439(00)00071-X.

[22] J. Świetlik, E. Sikorska, Application of fluorescence spectroscopy in the studies of natural organic matter fractions reactivity with chlorine dioxide and ozone, Water Res. 38 (2004) 3791–3799.

[23] X. Zhang, J. Shen, X. Huo, J. Li, Y. Zhou, J. Kang, Z. Chen, W. Chu, S. Zhao, L. Bi, X. Xu, B. Wang, Variations of disinfection byproduct precursors through conventional drinking water treatment processes and a real-time monitoring method, Chemosphere 272 (2021) 129930, https://doi.org/10.1016/j.chemosphere.2021.129930.

[24] K. Watson, M.J. Farré, F.D.L. Leusch, N. Knight, Using fluorescence-parallel factor analysis for assessing disinfection by-product formation and natural organic matter removal efficiency in secondary treated synthetic drinking waters, Sci. Total Environ. 640–641 (2018) 31–40, https://doi.org/10.1016/j.scitotenv.2018.05.280.

[25] E. Fernández-Pascual, B. Droz, J. O'Dwyer, C. O'Driscoll, E.H. Goslan, S. Harrison, J. Weatherill, Fluorescent dissolved organic matter components as surrogates for disinfection byproduct formation in drinking water: a critical review, ACS ES&T Water 3 (2023) 1997–2008, https://doi.org/10.1021/acsestwater.2c00583.

[26] E.N. Hidayah, Y.C. Chou, H.H. Yeh, Comparison between HPSEC-OCD and F-EEMs for assessing DBPs formation in water, J. Environ. Sci. Heal. - Part A Toxic/Hazardous Subst. Environ. Eng. 52 (2017) 391–402, https://doi.org/10.1080/10934529.2016.1262607.

[27] P. Jutaporn, W. Laolertworakul, K. Tungsudjawong, W. Khongnakorn, S. Leungprasert, Parallel factor analysis of fluorescence excitation emissions to identify seasonal and watershed differences in trihalomethane precursors, Chemosphere 282 (2021) 131061, https://doi.org/10.1016/j.chemosphere.2021.131061.

[28] C. Ma, H. Xu, L. Zhang, H. Pei, Y. Jin, Use of fluorescence excitation–emission matrices coupled with parallel factor analysis to monitor C- and N-DBPs formation in drinking water recovered from cyanobacteria-laden sludge dewatering, Sci. Total Environ. 640–641 (2018) 609–618, https://doi.org/10.1016/j.scitotenv.2018.05.369.

[29] N.M. Peleato, R.C. Andrews, Comparison of three-dimensional fluorescence analysis methods for predicting formation of trihalomethanes and haloacetic acids, J. Environ. Sci. (China) 27 (2015) 159–167, https://doi.org/10.1016/j.jes.2014.04.014.

[30] H.V.M. Nguyen, H.S. Lee, S.Y. Lee, J. Hur, H.S. Shin, Changes in structural characteristics of humic and fulvic acids under chlorination and their association with trihalomethanes and haloacetic acids formation, Sci. Total Environ. 790 (2021) 148142, https://doi.org/10.1016/j.scitotenv.2021.148142.

[31] Y. Wang, L. Li, Z. Sun, H. Dong, J. Yu, Z. Qiang, Removal of disinfection by-product precursors in drinking water treatment processes: is fluorescence parallel factor analysis a promising indicator? J. Hazard. Mater. 418 (2021) 126298 https://doi.org/10.1016/j.jhazmat.2021.126298.

[32] D. Ma, C. Xia, B. Gao, Q. Yue, Y. Wang, C-, N-DBP formation and quantification by differential spectra in MBR treated municipal wastewater exposed to chlorine and chloramine, Chem. Eng. J. 291 (2016) 55–63, https://doi.org/10.1016/j.cej.2016.01.091.

[33] A. Ignatev, T. Tuhkanen, Step-by-step analysis of drinking water treatment trains using size-exclusion chromatography to fingerprint and track protein-like and humic/fulvic-like fractions of dissolved organic matter, Environ. Sci.: Water Res. Technol. 5 (2019) 1568–1581, https://doi.org/10.1039/c9ew00340a.

[34] M. Vera, S. Cruz, M.R. Boleda, J. Mesa, J. Martín-Alonso, S. Casas, O. Gibert, J.L. Cortina, Fluorescence spectroscopy and parallel factor analysis as a dissolved organic monitoring tool to assess treatment performance in drinking water trains, Sci. Total Environ. 584–585 (2017) 1212–1220, https://doi.org/10.1016/j.scitotenv.2017.01.184.

[35] M. Abenza, J. Rodríguez, M. Fernández de Labastida, J. de Pablo, J.L. Cortina, V. Martí, E. Vázquez-Suñé, O. Gibert, Reclamation of urban pollution impacted groundwater by advanced treatment processes: effect of prechlorination on the removal of metals, ammonium and NOM at pilot scale, J. Water Process Eng. 54 (2023) 103973, https://doi.org/10.1016/j.jwpe.2023.103973.

[36] C.J. Williams, D. Conrad, D.N. Kothawala, H.M. Baulch, Selective removal of dissolved organic matter affects the production and speciation of disinfection byproducts, Sci. Total Environ. 652 (2019) 75–84, https://doi.org/10.1016/j.scitotenv.2018.10.184.

[37] J. Jiang, X. Zhang, X. Zhu, Y. Li, Removal of intermediate aromatic halogenated DBPs by activated carbon adsorption: a new approach to controlling halogenated DBPs in chlorinated drinking water, Environ. Sci. Technol. 51 (2017) 3435–3444, https://doi.org/10.1021/acs.est.6b06161.

[38] A.A. Cuthbertson, S.Y. Kimura, H.K. Liberatore, R.S. Summers, D.R.U. Knappe, B.D. Stanford, J.C. Maness, R.E. Mulhern, M. Selbes, S.D. Richardson, Does granular activated carbon with chlorination produce safer drinking water? From disinfection byproducts and total organic halogen to calculated toxicity, Environ. Sci. Technol. 53 (2019) 5987–5999, https://doi.org/10.1021/acs.est.9b00023.

[39] N. Fischer, A. Ghosh, B. Talabi, C. Seidel, P. Westerhoff, Chlorine addition prior to granular activated carbon contactors improves trihalomethane control, AWWA Water Sci. 1 (2019), https://doi.org/10.1002/aws2.1119 n.pag.

[40] C.U. Erdem, A. Mohamed, C. Liu, T. Karanfil, Activated carbon and organic matter characteristics impact the adsorption of DBP precursors when chlorine is added prior to GAC contactors, Water Res. 184 (2020) 116146, https://doi.org/10.1016/j.watres.2020.116146.

[41] L. Ponce-Robles, B. Masdemont-Hernández, T. Munuera-Pérez, A. Pagán-Muñoz, A.J. Lara-Guillén, A.J. García-García, F. Pedrero-Salcedo, P.A. Nortes-Tortosa, J.J. Alarcón-Cabañero, WWTP effluent quality improvement for agricultural reuse using an autonomous prototype, Water 12 (2020) 2240, https://doi.org/10.3390/w12082240.

[42] K.R. Murphy, C.A. Stedmon, P. Wenigd, R. Bro, OpenFluor– an online spectral library of auto-fluorescence by organic compounds in the environment, Anal. Methods-UK 6 (2014) 658–661, https://doi.org/10.1039/c3ay41935e.

[43] S.A. Baghoth, S.K. Sharma, G.L. Amy, Tracking natural organic matter (NOM) in a drinking water treatment plant using fluorescence excitation-emission matrices and PARAFAC, Water Res. 45 (2011) 797–809, https://doi.org/10.1016/j.watres.2010.09.005.

[44] S. Shao, H. Liang, F. Qu, H. Yu, K. Li, G. Li, Fluorescent natural organic matter fractions responsible for ultrafiltration membrane fouling: identification by adsorption pretreatment coupled with parallel factor analysis of excitation–emission matrices, J. Membr. Sci. 464 (2014) 33–42, https://doi.org/10.1016/j.memsci.2014.03.071.

[45] M. Park, S.A. Snyder, Sample handling and data processing for fluorescent excitation-emission matrix (EEM) of dissolved organic matter (DOM), Chemosphere 193 (2018) 530–537, https://doi.org/10.1016/j.chemosphere.2017.11.069.

[46] O. Gibert, B. Lefèvre, M. Fernández, X. Bernat, M. Paraira, M. Pons, Fractionation and removal of dissolved organic carbon in a full-scale granular activated carbon filter used for drinking water production, Water Res. 47 (2013) 2821–2829, https://doi.org/10.1016/j.watres.2013.02.028.

[47] M. Philibert, S. Luo, L. Moussanas, Q. Yuan, E. Filloux, F. Zraick, K.R. Murphy, Drinking water aromaticity and treatability is predicted by dissolved organic matter fluorescence, Water Res. 220 (2022) 118592, https://doi.org/10.1016/j.watres.2022.118592.

[48] T. Bond, E.H. Goslan, S.A. Parsons, B. Jefferson, A critical review of trihalomethane and haloacetic acid formation from natural organic matter surrogates, Environ. Technol. Rev. 1 (2012) 93–113, https://doi.org/10.1080/09593330.2012.705895.

[49] T. Zeng, C.J. Wilson, W.A. Mitch, Effect of chemical oxidation on the sorption tendency of dissolved organic matter to a model hydrophobic surface, Environ. Sci. Technol. 48 (2014) 5118–5126, https://doi.org/10.1021/es405257b.

[50] M. Bahram, R. Bro, C. Stedmon, A. Afkhami, Handling of Rayleigh and Raman scatter for PARAFAC modeling of fluorescence data using interpolation, J. Chemometr. 20 (2006) 99–105, https://doi.org/10.1002/cem.978.

[51] T. Maqbool, Y. Qin, Q.V. Ly, J. Zhang, C. Li, M.B. Asif, Z. Zhang, Exploring the relative changes in dissolved organic matter for assessing the water quality of full-scale drinking water treatment plants using a fluorescence ratio approach, Water Res. 183 (2020) 116125, https://doi.org/10.1016/j.watres.2020.116125.

[52] C. Fang, X. Luan, F. Ao, X. Wang, S. Ding, Z. Du, S. Liu, R. Jia, W. Chu, Decomposition of total organic halogen formed during chlorination: the iceberg of halogenated disinfection byproducts was previously underestimated, Environ. Sci. Technol. 57 (2023) 1433–1442, https://doi.org/10.1021/acs.est.2c03596.

[53] C. Chen, X. Zhao, H. Chen, J. Wang, Y. Wang, Q. Xian, The investigation of quenching conditions for the analysis of total organic halogen, aliphatic and aromatic halogenated disinfection byproducts formed from chlor(am)ination, J. Hazard. Mater. 475 (2024) 134918, https://doi.org/10.1016/j.jhazmat.2024.134918.

[54] L. Chen, W.-E. Zhuang, L. Yang, Critical evaluation of the interaction between fluorescent dissolved organic matter and Pb(II) under variable environmental conditions, Chemosphere 307 (2022) 135875, https://doi.org/10.1016/j.chemosphere.2022.135875.
[55] B.A. Poulin, J.N. Ryan, G.R. Aiken, Effects of iron on optical properties of dissolved organic matter, Environ. Sci. Technol. 48 (2014) 10098–10106, https://doi.org/10.1021/es502670r.
[56] N. Mladenov, A. Bigelow, B. Pietruschka, M. Palomo, C. Buckley, Using submersible fluorescence sensors to track the removal of organic matter in decentralized wastewater treatment systems (DEWATS) in real time, Water Sci. Technol. 77 (2018) 819–828, https://doi.org/10.2166/wst.2017.573.